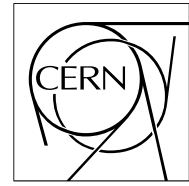


The Compact Muon Solenoid Experiment

CMS Note

Mailing address: CMS CERN, CH-1211 GENEVA 23, Switzerland



September 1, 2000

A model for the CMS tracker analog optical link

Th.Bauer

Institute of Highenergy Physics, Vienna, Austria

F.Vasey

CERN, Geneva, Switzerland

Abstract

A model of the CMS-tracker analog optical link has been developed based on experimental and theoretical data as well as on the projected performance of the final link components. This model includes a monte-carlo module capable of simulating the effects of component tolerances on system characteristics. Using this model it is possible to predict the signal-to-noise and gain performance of various link configurations. The results indicate that the final version of the analog optical link will satisfy the system specifications. In particular they confirm that the spread of system-gain caused by component tolerances can be successfully compensated for by introducing a laser driver with switchable gain.

1 Introduction

The data acquisition system for the tracker of the Compact Muon Solenoid (CMS) experiment will make use of approximately 50000, 100 m long, analog optical fiber links to read-out the detector signals processed by the front-end electronics [1] [2]. A block diagram of the CMS tracker frontend electronics system is illustrated in Fig.1.

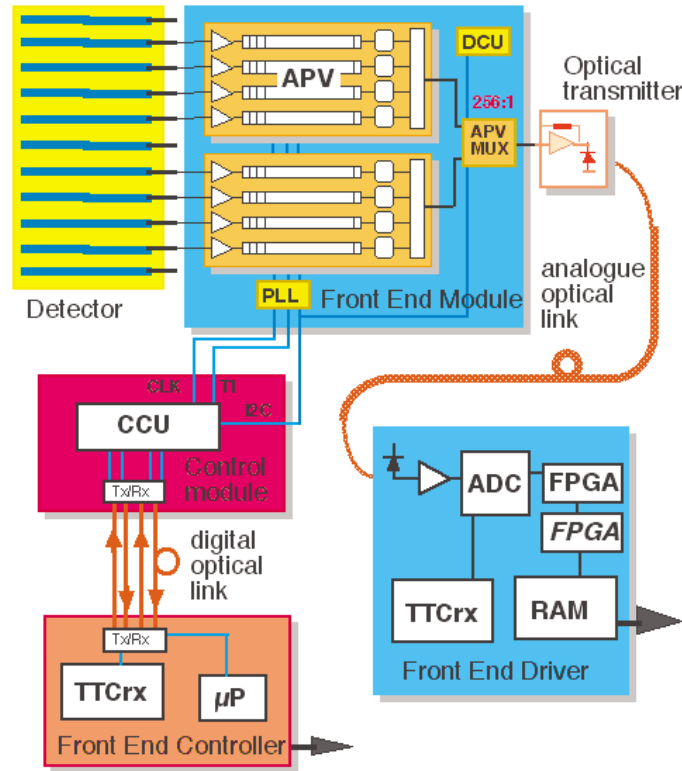


Figure 1: block diagram of the CMS-tracker electronics

The analog optical links are based on edge-emitting laser transmitters and pin photodiode receivers operating at a wavelength of 1310 nm. In every fiber 256 detector channels are time-multiplexed at a rate of 40Msamples/s. [3]

Meeting the electrical constraints given by the design of the APV and Multiplexer (MUX) outputs and of the front end driver (FED) ADC input range, the optical link gain must be chosen so as to optimize dynamic range while minimizing its contribution to the overall system noise. This optimisation must take into account component tolerances.

A four-channel optical link prototype was released in 1998 to demonstrate the performance of the analog optical readout chain. This prototype has been thoroughly evaluated [4] [5] in the laboratory and in a testbeam setup demonstrating performance well within specifications. Since the design of the four-channel analog optical link prototype, the boundary conditions set by the readout electronics have changed. The new readout chip APV25 [6] offers a higher output signal and the FED ADC input range was reduced.

In order to meet these new constraints while maintaining good analog performance, the gain distribution of the optical link had to be modified. In particular the total link-gain had to be lowered from 2 to 0.8. Also the laser-driver chip was redesigned in a deep submicron technology and this opportunity was used to modify its

specifications. The new version will feature a reduced noise as well as the ability to vary the driver-gain in four steps so as to compensate the large spread of the system-gain caused by component tolerances.

To help predict the performance of the final version of the analog optical link, a noise model has been developed, based on experimental data collected with the four-channel prototypes and on the expected performance of the new components. Using this model, the influence of each link component on the signal-to-noise ratio has been investigated, and the gain distribution along the optical chain has been optimized for best results. Moreover, to investigate in detail the effect of component tolerances on system performance, a monte carlo simulation module was also included.

The model is built in such a way that components characteristics can easily be modified or added. Thus, the effect of future link-configurations on signal-to-noise and gain can easily be investigated in a short time.

2 Model

2.1 Description

The components of the analog optical link have been characterized by the manufacturers and by CMS groups. [7] [8] [9]. Based on the availability of this experimental data, a link model has been developed consisting of five blocks, as shown in Fig.2.

Each block is described by its gain and noise function. The noise functions are dependent on components parameters such as gain, bias-current and optical power level, and have been approximated to fit the available experimental data.

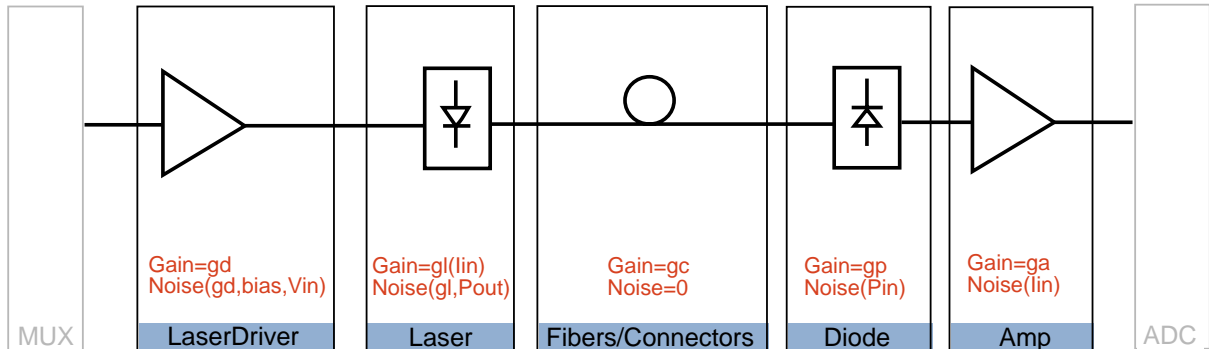


Figure 2: Block diagram of the optical link model consisting of noise functions and gains

Assuming the noise sources to be added to the output of each system block, the noise contribution of each component, referred to the output of the link can be written as:

$$N_{output_i} = N_i \prod_{j>i} G_j$$

The total noise is therefore:

$$N_{total} = \sqrt{\sum (N_{output_i})^2}$$

And the total gain of the system can be evaluated as:

$$G_{total} = \prod_i G_i$$

In a first step, the output characteristics of the existing analog optical link prototype have been simulated and compared to the experimental results, proving the reliability of the model. The model was then used to test future link configurations and to investigate the influence of various gain distributions on the dynamic range and signal-to-noise performance of the link. Finally monte carlo simulations were carried out to investigate the performance-spread induced by component tolerances, and the effect of laser driver gain switching.

2.2 Toleranced Gain Distributions

An optical link, even if it is considered as one lumped element, is in fact a chain of optical components with their own characteristics and tolerances. In a system with 50000 fibres, precise trimming or sorting of these components to achieve homogeneous performance is impractical. A toleranced system analysis thus needs to be performed to guarantee satisfactory link characteristics in all cases, while ensuring that reasonable manufacturing tolerances are specified to components suppliers.

The optical link gain is constrained by the front-end chip output range (0 to 600mV) and the FED ADC input range (1V, 10bits). Its dynamic range is chosen so that each 8 bit data byte transmitted by the FED to the data acquisition (DAQ) system corresponds typically to a 3 MIP signal. The use of a 10 bit ADC when only 8 bits of processed data are transferred to the DAQ system allows to cope with large variations and inhomogeneities of gain, common mode, and working point. Knowing the APV chip sensitivity (100mV/MIP) and the ADC resolution (250mV/8bits), the typical optical link gain should thus be optimized around $G=0.8$.

The way this total gain is distributed among individual components is a compromise between device feasibility, and optimization of signal to noise ratio: whereas laser efficiency, photodiode responsivity and connector insertion loss are essentially dictated by industrial production constraints, the gains of laser driver and receiving amplifiers have been designed so as to reach the highest possible gain at the front-end of the link.

The resulting distribution of gains and tolerances is shown in Fig. 3.

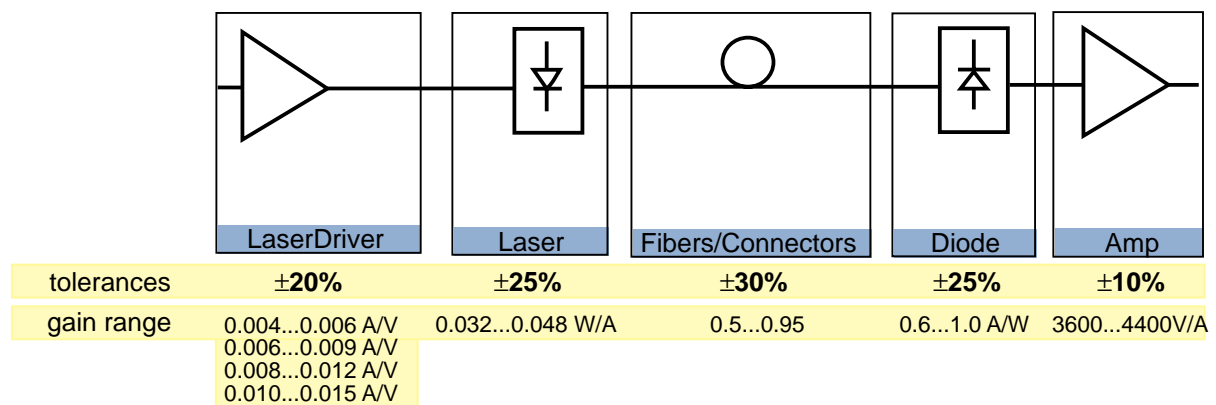


Figure 3: Assumed tolerances and gains for the monte-carlo simulation

The purpose of the model is now to confirm that the optical link performance is achieved not only in the typical case, but also at the edges of the gain distribution.

2.3 Monte Carlo Simulation

To simulate the performance spread of the whole system, the gain distribution of each component in the chain has to be taken into account. However, since the final components have not yet been chosen, no information on the real distributions of the component tolerances is available.

The component gains have thus been assumed to be uniformly distributed within the given specification range in a pessimistic worst case scenario. Fig. 4 shows for instance the distribution assumed for the laser.

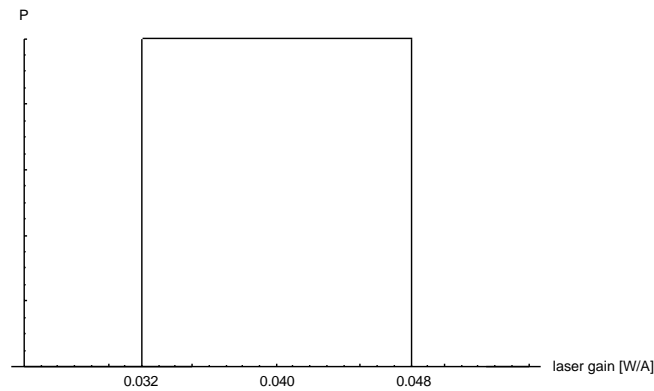


Figure 4: Uniform distribution within specification range assumed for the laser

The case of the laser driver is more complex since we need to include the ability to switch its gain in four steps. The four gains of one driver chip are toleranced in such a way that in case of a „low gain“ driver chip all four available gains are lower than the typical value and in the case of a „high gain“ driver all four gains are above the typical value. This is done using a laser-driver gain seed distribution assumed around the average gain of the laser driver (Fig. 5a).

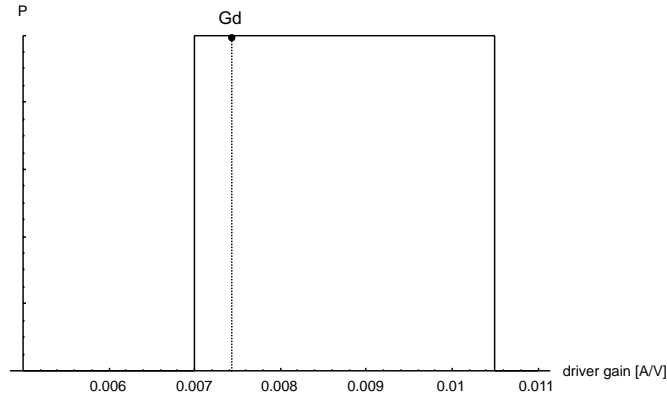


Figure 5a: Choosing one sample out of a seed laser driver gain distribution

For each driver chip in a link sample, the four correlated gains Gd-a to Gd-d (Fig.5b) are generated by scaling each randomly chosen Gd (Fig. 5a) using four constant factors.

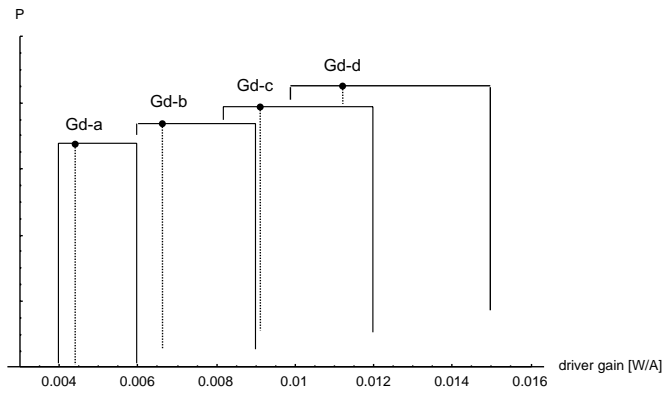


Figure 5b: Correlated distributions of all four driver gains by scaling the seed distribution (Fig.5.a) with constant factors

The multiplicative effect of all component tolerances induces a huge spread on the system-gain. To evaluate the gain distribution of the system, the simulation uses one million sample links. For each sample link a set of five sample gains (one for each system block) is taken out of the source distributions.

The total gain of each sample link is calculated for each of the four possible laser-driver gains. The driver gain achieving the total gain closest to 0.8 is then chosen, thus optimizing system gain.

Optimizing the system to a given gain-value is only one possibility. The driver switching algorithm can become much more complex and for instance also take S/N maximisation into account.

3 Results

3.1 Gain

Simulating the gain spread of the analog optical link using only one typical driver gain of 10mS tolerated from 8 mS...12 mS ($\pm 20\%$) illustrates well the huge spread (almost an order of magnitude) induced by the combination of realistic component tolerances. (Fig. 6)

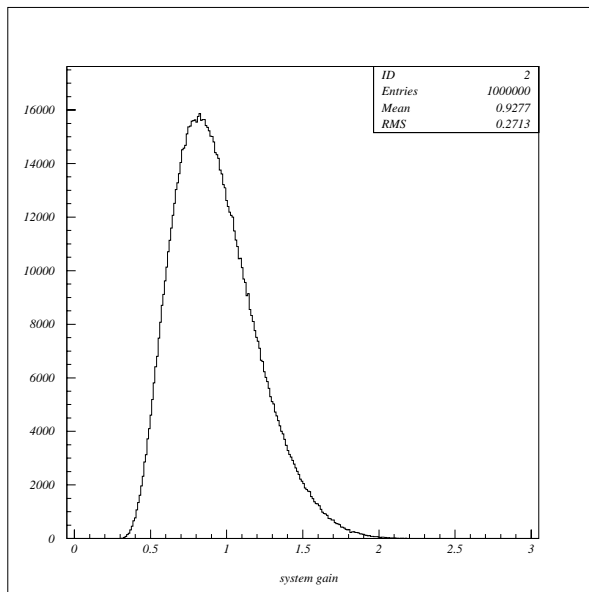


Figure 6: System gain distribution using only one driver gain

The shape of the system gain distribution is asymmetric due to the fact that the source distributions are not symmetric around zero and that the function generating the final distribution is a product, not a sum. The final gain distribution would be symmetric on a logarithmic scale, but not on a linear scale.

By introducing the switchable laser driver gain into the simulation, the gain distribution of the system can be significantly narrowed (Fig. 7).

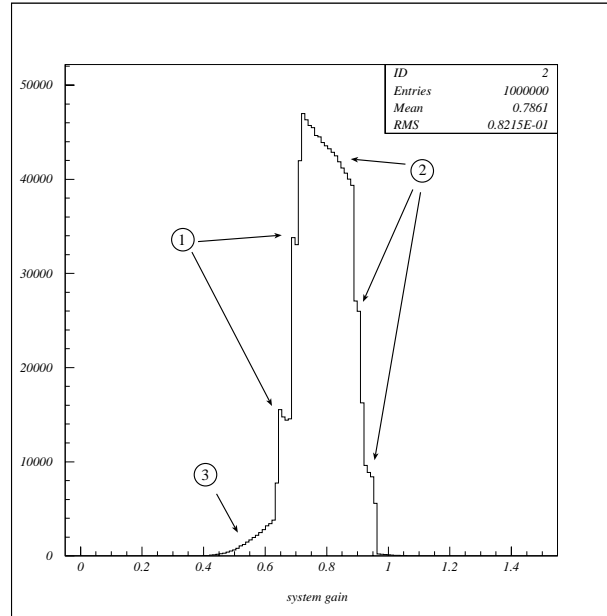


Figure 7: Sytem gain distribution using all four driver gains for optimisation

The driver-switching process can be roughly imagined as slicing the „single driver gain“ - distribution (Fig. 6) into four slices and centering them on the x-axis around 0.8. Thus the kinks of the distribution ((1) in Fig.7) can be identified as the borders of the slices while the remaining parts of the original slope are also visible ((2) in Fig 7). The tail on the low gain side of the distribution ((3) in Fig. 7) contains the links of very low gain that could not be compensated with the available driver gain range. It is clearly visible that the driver gain range compensates high-gain cases better than low-gain cases.

The shape of the histogram is strongly dependent on the individual source distributions and on the applied switching algorithm. In particular the magnitude of the uncompensated tail ((3) in Fig. 7) also depends strongly on these assumptions and is vastly exaggerated in this worst case example with uniform distributions. Trials with arbitrarily chosen gaussian distributions have confirmed this fact, and we conclude that the tails do not deserve further discussion before the exact distributions are known.

Table 1: Summary of the range of system gains

gain spread					
	sigma (RMS)		<i>min</i>	<i>mean</i>	<i>max</i>
without switching	0.27	full range	0.28	0.93	2.41
		98%	0.28	0.93	1.58
with switching	0.08	full range	0.35	0.79	1.20
		98%	0.60	0.79	0.98

Tab. 1 summarizes the results of the monte-carlo simulation, showing the full range and the range containing 98% of the links (around mean value) for both unswitched and switched cases. The full ranges are evaluated by calculating the product of the max/min border values of all source distributions and, when using the switchable driver, compensating with the corresponding worst case driver gain. The full range is not visible in the histograms because the border values are too improbable, but would have to be taken into account when issuing system specifications.

The ratio of max/min gain has been reduced from 8.6 to 3.4 using the new laser driver with switchable gain. Moreover, in 98% of the cases, the link gain will fall in a $\pm 25\%$ window around the desired value of 0.8.

The impact of the gain compensation on the system output range is well illustrated in Fig. 8. The black lines mark the min/max cases of output voltage vs. input voltage for links with one driver gain whereas the dark gray lines mark the min/max cases for links where the tolerance compensation has been applied. The (innermost) light gray lines illustrate the range where 98% of the links fall in the compensated case. The typical gain of 0.8 is indicated by the dashed line.

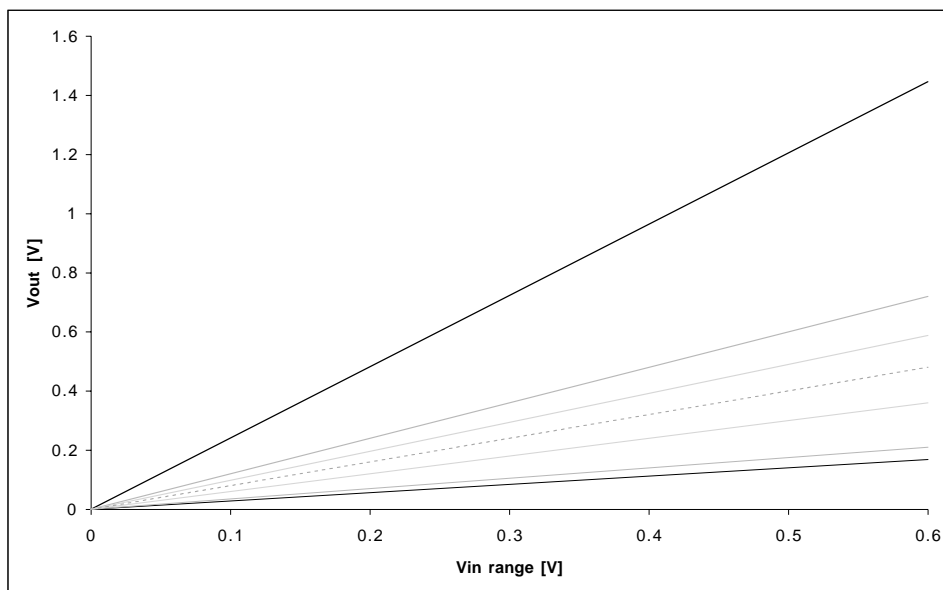


Figure 8: Output voltage vs. input voltage for min/max cases

Again, it becomes visible that the adjustable driver compensates high-gain links more than low-gain links. This asymmetry is however dependent on the individual component distribution and on the choice of target gain for the whole link.

Fig.9 is the same as Fig. 8 but this time showing FED ADC bits vs. input voltage. In the switched-gain case, the frontend chip output range (600mV) is well mapped to the FED-ADC 10 bit range. In 98% of the cases, almost one most significant bit is left free to accommodate working point fluctuations and common mode effects. The online data processing electronics of the FED will perform pedestal and common mode subtraction before outputting an 8 bit word to the DAQ system. Fig. 9 indicates that 8 bits will typically correspond to a signal of 320 mV (3.2 MIPS). In 99% of the cases, signals $\leq 0.26\text{V}$ (2.6 MIPS) will be transmitted to the DAQ with 8 bit resolution, without being clipped.

Fig.10 illustrates the typical usage of optical link operating range with V_{baseline} determined by the APV working point and pedestal, and V_{bias} representing the laser working point. An 8 bit range above the working points is highlighted, corresponding to a 320mV input signal being transferred to the DAQ system.

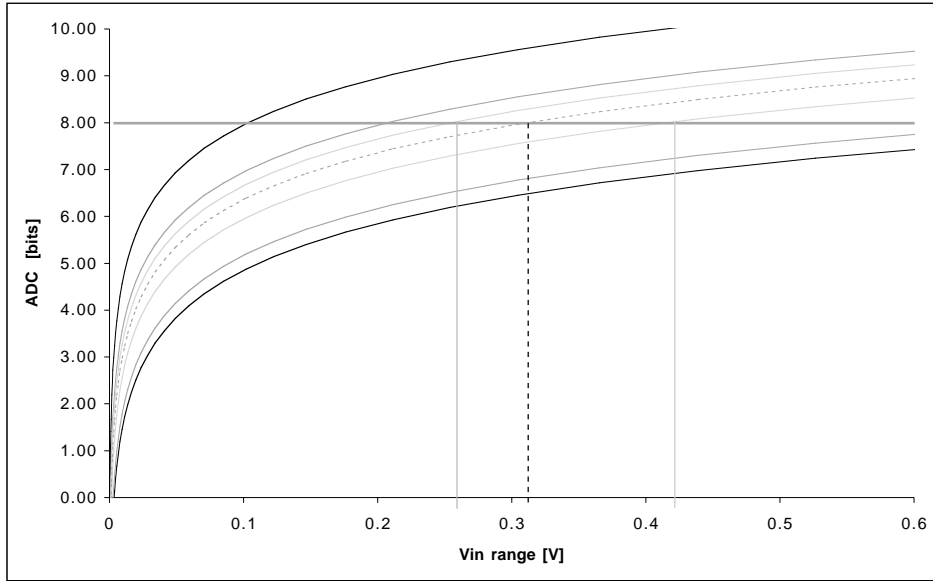


Figure 9: ADC bits vs. input voltage for min/max cases.

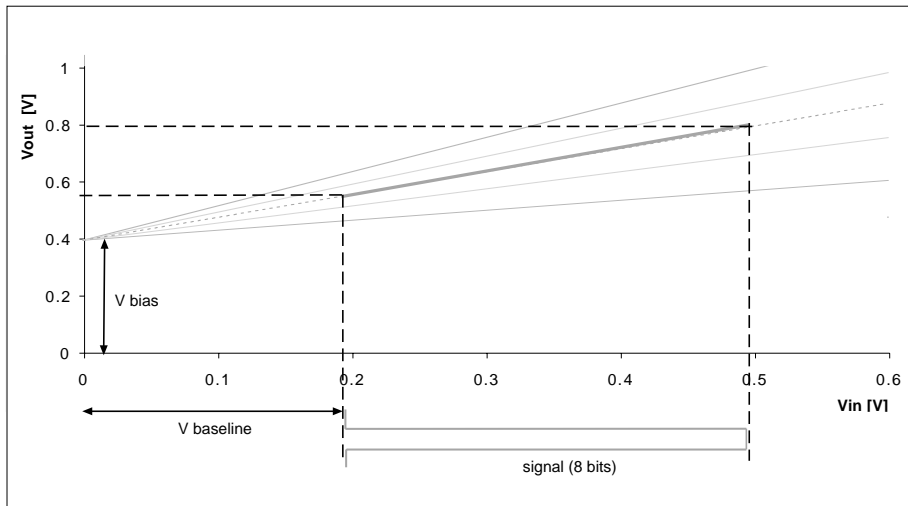


Figure 10: typical usage of the operating range (switched driver case)

3.2 Signal to noise ratio

The noise behaviour of the link has been simulated using noise functions that are approximations to measured and simulated data. The final components are not all available for evaluation and the data on their noise behaviour is preliminary. For a more precise description of the lasers Relative Intensity Noise (RIN) function, which is dominating the total noise of the link, more detailed data would be needed. Ageing and radiation damage effects which will probably result in a higher laser bias current are not included in this first simulation. Furthermore the noise function assumed for the final laser driver chip is yet only based on a circuit simulation.

To ensure its reliability, the noise-model was first tested and refined by simulating the 4-channel prototype and

comparing the results to the measured noise values. Fig. 11 illustrates well that the results of the noise-model are in good agreement with the measurements.

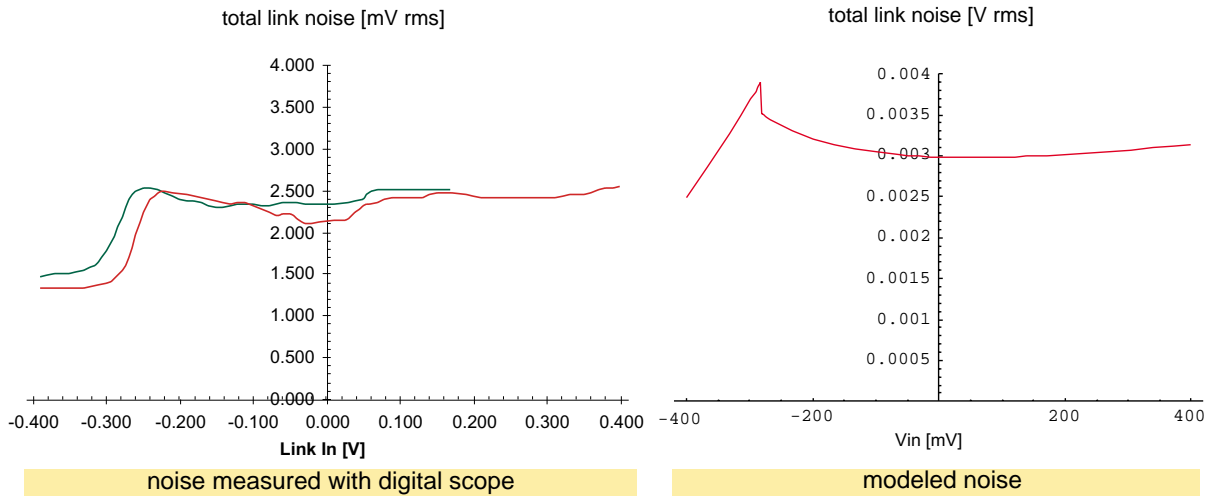


Figure 11: comparison between measured and modeled noise

Simulating the final link using the available data and assuming a peak input signal of 600 mV (6 MIPS) the model predicts a typical signal-to-noise ratio of 52 dB.

Due to the fact that the contribution of the individual components to the total noise are all different and partly nonlinear, the impact of the gain distributions to the total noise is rather complicated. Thus, it is of interest to combine the noise-simulation with the monte-carlo simulation of the component gains. By evaluating the peak signal-to-noise ratio for each of the monte carlo simulated links, the peak signal-to-noise distribution of the links can be investigated (Fig12). The results are summarized in Tab. 2.

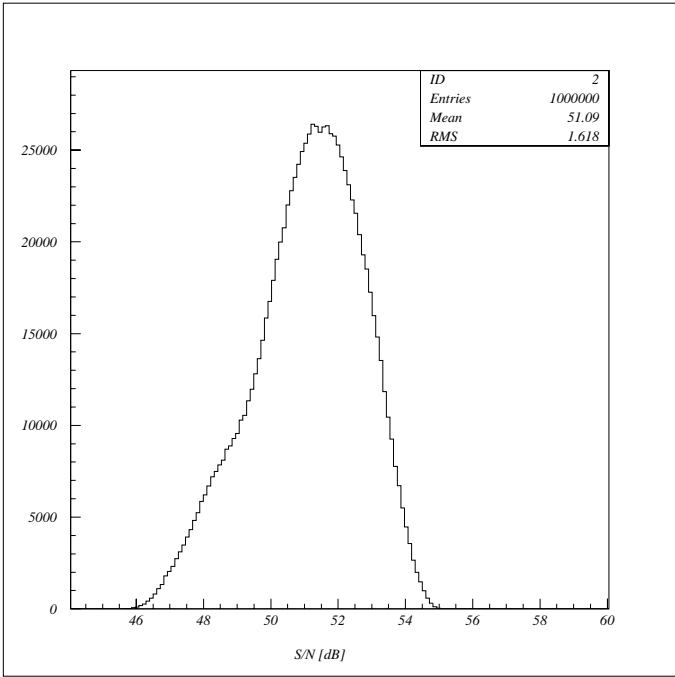


Figure 12: Signal-to-Noise distribution of the system (switched driver case)

The shape of the switched gain distribution (Fig.7) does not reappear in Fig.12 because links with different gains

can have the same signal-to-noise ratio and thus the distinctive features of the gain distribution are blurred in Fig.12.

Again, the characteristics of this distribution are very dependent on the assumed source distributions for the components gains. In particular applying an advanced driver switching algorithm, which would also include S/N maximisation, would probably lead to a narrower and upshifted distribution. Further investigations on the algorithm used for choosing the driver gain could be suggested once the final components have been selected.

Table 2: Summary of the systems signal-to-noise range

Peak-Signal-to-noise performance			
	<i>min</i>	<i>mean</i>	<i>max</i>
full range	45.5dB	51dB	55dB
highest 98%	47.4dB		55dB

4 Conclusions

A model of the CMS-tracker analog optical link has been developed and used to predict the gain and signal-to-noise performance of the readout system, including the impact of component tolerances.

The results show that the link will perform well within specifications. In particular the huge gain spread can successfully be compensated for, by introducing a new laser driver with switchable gain. The output range of the system will now in all cases map the FED ADC input range.

The simulated signal-to-noise distribution shows that the analog performance of the link will be maintained in the final design.

Once updated information on the characteristics of the finally chosen components becomes available, further investigation of the link performance can easily be performed. In particular the possibility of optimizing the performance of the link by using advanced switching algorithms for the laser driver should be examined.

References

- [1] CMS: The Tracker Project. Technical Design Report, CERN/LHCC 98-6, CMS TDR 5, April 1998.
- [2] G.Hall, „Analogue optical data transfer for the CMS tracker, Nuclear Instruments and Methods in Physics Research A 386 (1997) 138-142
- [3] F. Vasey, C. Azevedo, G. Cervelli, K. Gill, R. Grabit, F. Jensen, „Optical links for the CMS Tracker“, Proc. of the fourth workshop on electronics for LHC experiments, Snowmass, 1999, pp. 175-179
- [4] F.Vasey, C.Aguilar, C.Azevedo, V. Arbet-Engels, G.Cervelli, K. Gill, R. Grabit, F. Jensen, C.Mommaert, P.Moreira and G.Stefanini, „A 4-cannel analogue optical link for the CMS-Tracker“, Proceedings from the 4th Workshop on electronics for LHC Experiments, Rome, pp. 344-348, 1998
- [5] Th. Bauer, M. Friedl „optical link evaluation“ , October 1999 <http://home.cern.ch/bauer>
- [6] Rutherford Appleton Laboratory, Instrumentation Department: <http://www.te.rl.ac.uk/med/>
- [7] G.Cervelli, V.Arbet-Engels, K.Gill, R.Grabit, C.Mommaert, G.Stefanini, F.Vasey, „Characterization of laser diodes for analog parallel optical links“, Testing, packaging, reliability and applications of semiconductor lasers IV, SPIE Vol. 3626B, 1999, pp. 202-207

- [8] F. Jensen, C.S Azevedo, L. Björkman, G.Cervelli, K.Gill, R.Grabit, F.Vasey, „Evaluation and selection of analogue optical links for the CMS tracker - methodology and application”, CMS Note 1999/074
- [9] G.Cervelli, V.Arbe-Engels, K.Gill, R.Grabit, C.Mommaert, G.Stefanini, F.Vasey, „A method for the static characterisation of the CMS Tracker analogue links”, CMS Note 1998/043